Supplementary Information (SI) for Journal of Materials Chemistry A.
This journal is © The Royal Society of Chemistry 2026

Electronic Supplementary Information

Synergistic Interfacial Evaporation and Electricity Generation Enabled by Fe-Co PBA Derived nature Sponges

Rongfu Peng[1,2△], Boheng Huang[3△], Xinfeng Zhu[1], Yingyi Li[2], Shangru Zhai[4*], Chaohai Wang[1*]

1.Henan Key Laboratory of Water Pollution Control and Rehabilitation Technology, School of Municipal and Environmental Engineering, Henan University of Urban Construction, Pingdingshan 467036, People's Republic of China. E-mails: chaohai@huuc.edu.cn

2.Faculty of Light Industry and Chemical Engineering, Dalian Polytechnic University, Dalian 116034, P.R. China

3.Henan University of Urban Construction, Pingdingshan 467036, People's Republic of China.

4.Zhejiang University of Science and Technology, Hangzhou 310023, People's Republic of China. E-mails: zhaisrchem@163.com

Note S1. Calculation of energy conversion efficiency

The energy conversion efficiency (η) is calculated by the formula:

$$\eta = m_e h_{LV} / C_{opt} P_0$$

$$h_{LV} = Q + h_v$$

$$Q = C(T_1 - T_0)$$

Where m_e refers to the evaporation rate, h_{LV} is the enthalpy change of the evaporation enthalpy of water passing from its liquid to the gaseous phase, P_0 is the nominal solar illumination power of one sun and C_{opt} is the optical concentration on the evaporator surface. h_{LV} consists of the latent heat of evaporation (h_v) and total enthalpy of sensible heat (Q), The specific heat capacity of water (C) is 4.18 J·g^{-1}. T_0 is the starting temperature at the beginning of the experiment and T_1 is the temperature at the end of it. Since sponge evaporators are almost completely hydrated during photothermal evaporation, the change in the enthalpy of evaporation is related only to the content of free and intermediate water. Therefore, dark evaporation experiments were conducted to estimate the true enthalpy of evaporation of water in composite sponge. Water and sponge evaporators with the same surface area were sealed in a dark container containing a saturated magnesium chloride solution (ambient temperature 25 °C). The equivalent enthalpy of evaporation of water in the sponge evaporator was calculated using the formula:

$$\Delta H_{vap} m_0 = \Delta H_{equ} m_g$$

where ΔH_{vap} is the evaporation latent heat of pure water (2256 J·g^{-1}), ΔH_{equ} is the evaporation latent heat of FCSC, m_0 refers to evaporation mass change of water (without evaporator) under the dark condition, m_g is the mass change of FCSC within the same environmental condition.

Note S2. Degradation of Phenol

The catalytic degradation experiment of FCSC (9.6g) was conducted using 50 mL of BPA solution (10 ppm) as the model pollutant. Under identical conditions, two pieces of FCSC were subjected to catalytic degradation experiments in stirred BPA solutions. Typically, prior to initiating xenon lamp illumination, FCSC was immersed in the BPA solution under dark conditions and magnetically stirred for 1 hour to achieve adsorption equilibrium. During this period, 1 mL samples were extracted at specific time points for testing. Subsequently, PMS was added to the reactor, and the xenon lamp (CEL-PE300L-3A, China) was activated to initiate the synergistic reaction between photocatalytically activated PMS and FCSC. Similarly, 1 mL samples were taken at specified intervals, the catalyst was separated by magnetic separation, and then quenched with 1 mL $Na_2S_2O_3 \cdot 5H_2O$ (20 mM). The supernatant and condensate was analyzed using liquid chromatography with an autosampler (LC5090Plus, China). LC5090Plus instru-ment equipped with a C18 reversed-phase column (5 μm, 4.6 mm × 150mm). The UV detector set at λ = 270 nm. 0.8 mL min^{-1} methanol and 0.2 mL min^{-1} water were used as mobile phases. Used FCSC materials were washed three times with anhydrous ethanol and deionized water, then dried in an oven for cyclic testing. The degradation efficiency (DE) and rate constant (k min^{-1}) of bisphenol A were calculated using the following equations:

$$DE = \left(\frac{C_t}{C_0}\right) \times 100\%$$

$$\ln \frac{C_t}{C_0} = -k_{obs} \bullet t$$

where C_t is the concentration of BPA in solution at t min ($mg \cdot L^{-1}$), C_0 is the concentration of BPA in the initial solution ($mg \cdot L^{-1}$), k_{obs} is the observed pseudo-first-order removal rate constant (min^{-1}) and t is the reaction time (min).

Experimental

Reagents and material

Natural sponge was collected from the Mediterranean Sea. All chemical reagents were of analytical grade and used as received. **Solvents**, including anhydrous ethanol (C_2H_6O, ≥99.5%), methanol (CH_3OH, ≥99.5%), and tert-butanol ($C_4H_{10}O$, ≥99.5%), were employed. The following reagents were purchased from **Shanghai Guoyao Chemical Reagent Co., Ltd.**: ferrous sulfate heptahydrate ($FeSO_4·7H_2O$, ≥99%). Reagents obtained from **Shanghai Macklin Biochemical Co., Ltd.** included: potassium cobalt cyanide ($C_6CoK_3N_6$, ≥99%), cobalt acetate tetrahydrate ($C_4H_6CoO_4·4H_2O$, ≥99.5%), polyvinylpyrrolidone K30 (PVP, ≥99%), and Phenol (C_6H_6O, ≥99%) was supplied by **Aladdin Chemical Co., Ltd**.

Preparation of FCSC

The nature sponge was cleaned by sequential ultrasonication in deionized water, ethanol, and again deionized water (15 min for each step), followed by drying. To functionalize the sponge with Fe and Co species, Solution A was prepared by dissolving 0.374 g of $C_4H_6CoO_4·4H_2O$ and 0.42 g of $FeSO_4·7H_2O$ in 200 mL of distilled water. Separately, Solution B was formed by dissolving 0.664 g of $C_6CoK_3N_6$ and 6 g of PVP in another 200 mL of distilled water. The dried sponge was first immersed in Solution A for 2 h to allow metal ion adsorption. Subsequently, it was transferred to Solution B and continuously stirred for 24 h to ensure thorough impregnation, yielding the precursor denoted as Fe–Co@Sponge (FCS). After drying, the FCS precursor was calcined at 900 °C for 3 h under a nitrogen atmosphere to obtain the final carbonized material, designated as Fe–Co@Sponge–C (FCSC), (Fig.S1b) which exhibited enhanced structural stability and functional properties.

characterization

The microstructure and elemental distribution of the samples were characterized using scanning electron microscopy (SEM, FEI Quanta 250F) equipped with energy-dispersive X-ray spectroscopy (EDS). The pore structure and specific surface area were determined by nitrogen adsorption–desorption measurements on a BET surface area analyzer (Micromeritics ASAP 2020). The crystal structures were investigated by X-ray diffraction (XRD, JEOL JSM-6360LV). Chemical bonds and functional groups were analyzed by Fourier-transform infrared spectroscopy (FTIR, Thermo Fisher Scientific Nicolet iS20), while molecular vibrations were studied by Raman spectroscopy (Renishaw). To evaluate their broadband solar absorption capability for photothermal applications, the UV–vis–NIR absorption spectra of the four sponge samples were recorded on a spectrophotometer (Shimadzu UV-3600i Plus).

Solar-driven water generation

The SDIWE system was mainly composed of a xenon lamp(CEL-PE300L-3A，China) and an electronic Analytical balance(ML802，0.0001g). Typically, The FCSC was placed on a foam board with absorbent paper at the bottom connected to a water source. (Fig. S9)

Design of the water-electricity co-generation based on the FCSC

The water-electricity co-generation illustrated in Fig. S2, conductive silver paste was applied to the top and bottom surfaces of the material and connected to copper foil wires. The conductive silver paste was prepared using silver powder as the conductive filler and acrylic resin as the binder, together with an appropriate amount of organic solvent. Specifically, a certain amount of acrylic resin was dissolved in ethanol (or isopropanol) and stirred thoroughly using a magnetic stirrer to form a homogeneous resin solution. Silver powder was then gradually added to this solution under continuous stirring to ensure uniform dispersion of the silver particles within the resin matrix. To further enhance the dispersion of silver powder and the uniformity of the paste, the resulting mixture was subjected to ultrasonication for 10–30 minutes. The final silver paste exhibited excellent rheological and conductive properties. The prepared paste was sealed for storage and lightly stirred before use to ensure homogeneity. For the moisture electricity generation measurement, the sample was placed in a sealed glass container, irradiated from above with a xenon lamp simulating sunlight, and connected via the conductive wires to a CHI760E electrochemical workstation (Shanghai) to record its electrical output. The sample was placed in a sealed glass container, irradiated from above with a xenon lamp simulating sunlight, and connected to an electrochemical workstation via wires to measure its electricity generation performance. During fabrication, a layer-by-layer PBA impregnation strategy was adopted to induce internal concentration gradients within the FCSC, which effectively enhances its electricity generation. All experiments were conducted using the FCSC samples with dimensions of 1 cm × 3 cm × 1 cm.

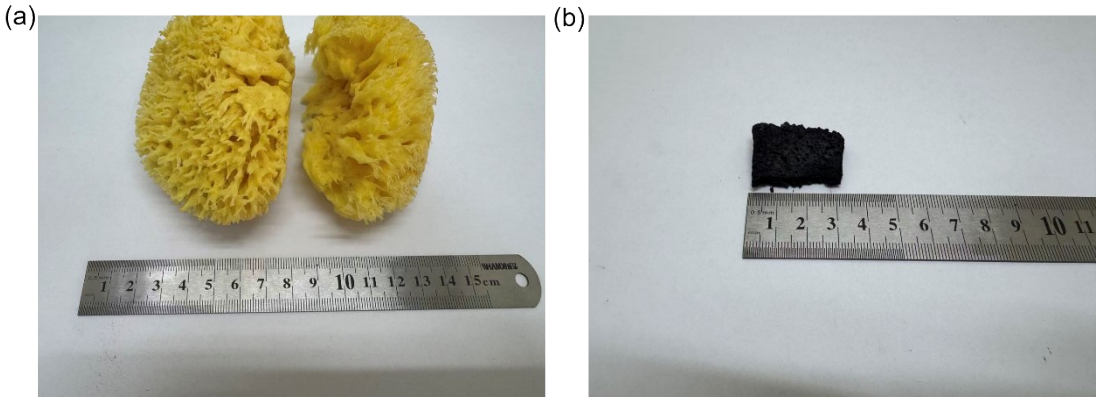

Figure S1. Natural Sponge Images and FCSC Images

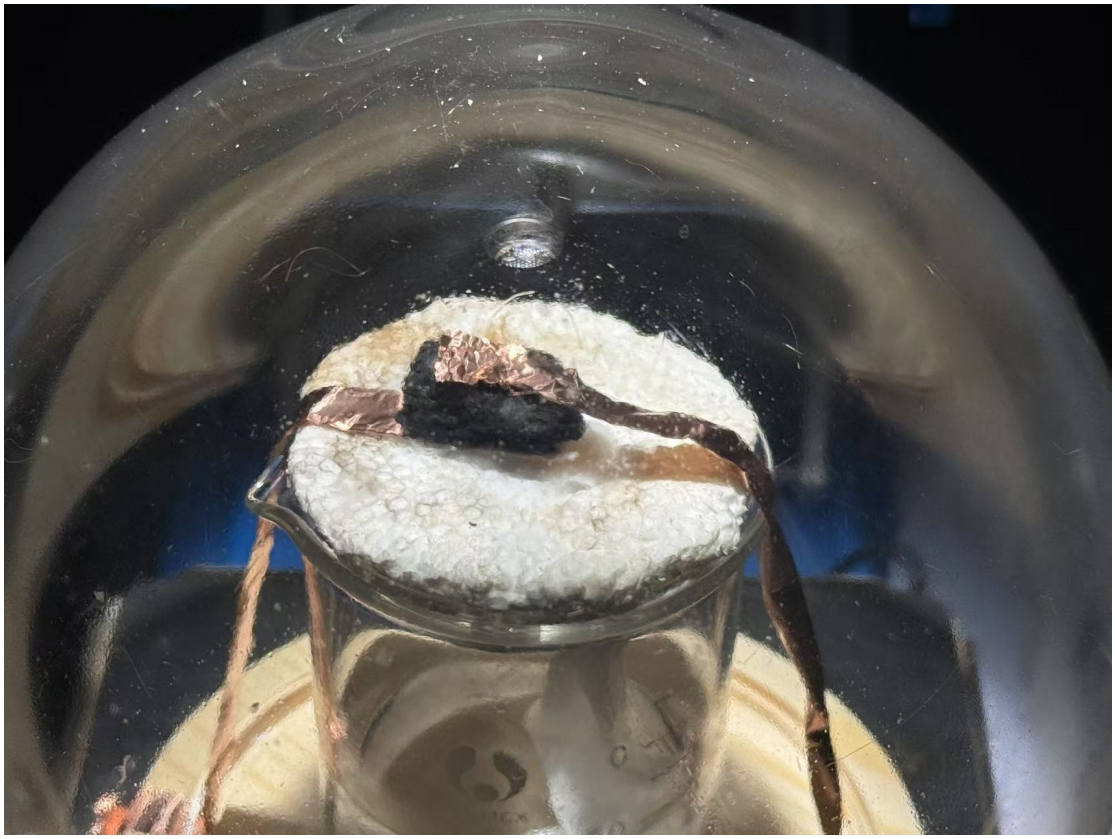

Figure S2. power generation system

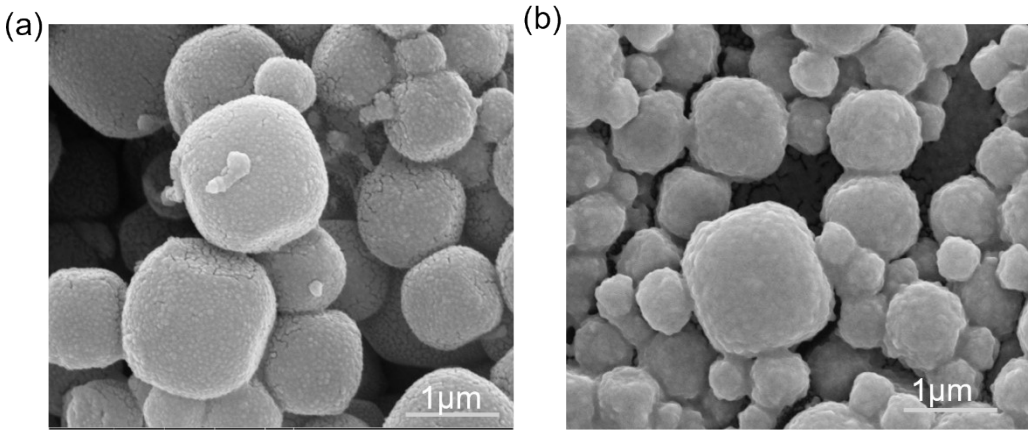

Figure S3.SEM image of the FCS(a) and FCSC(b)

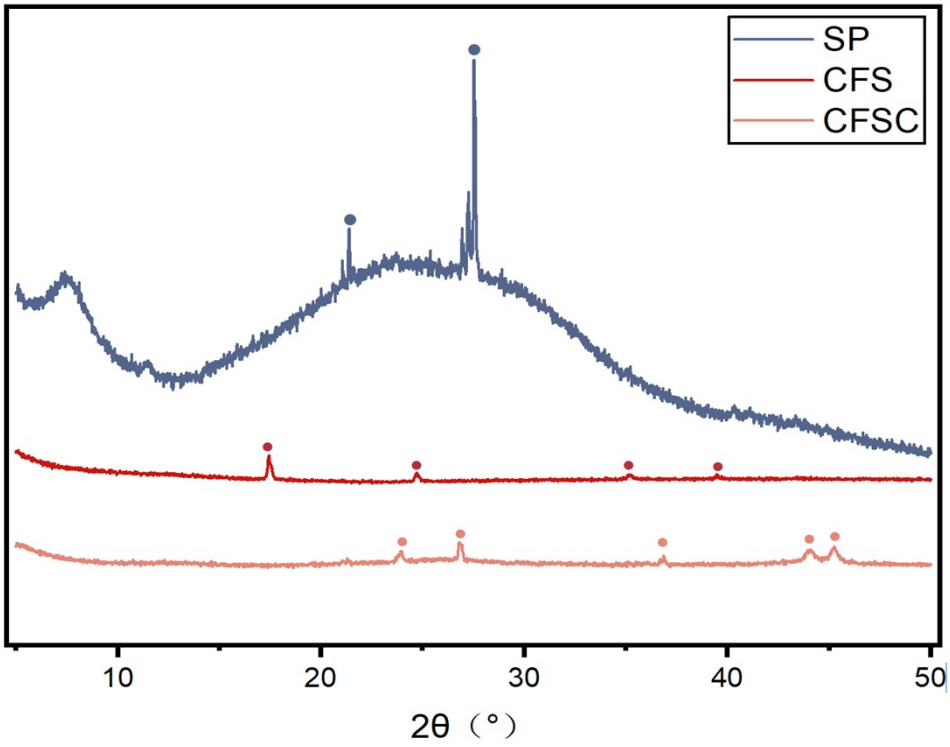

Figure S4. The XRD patterns.

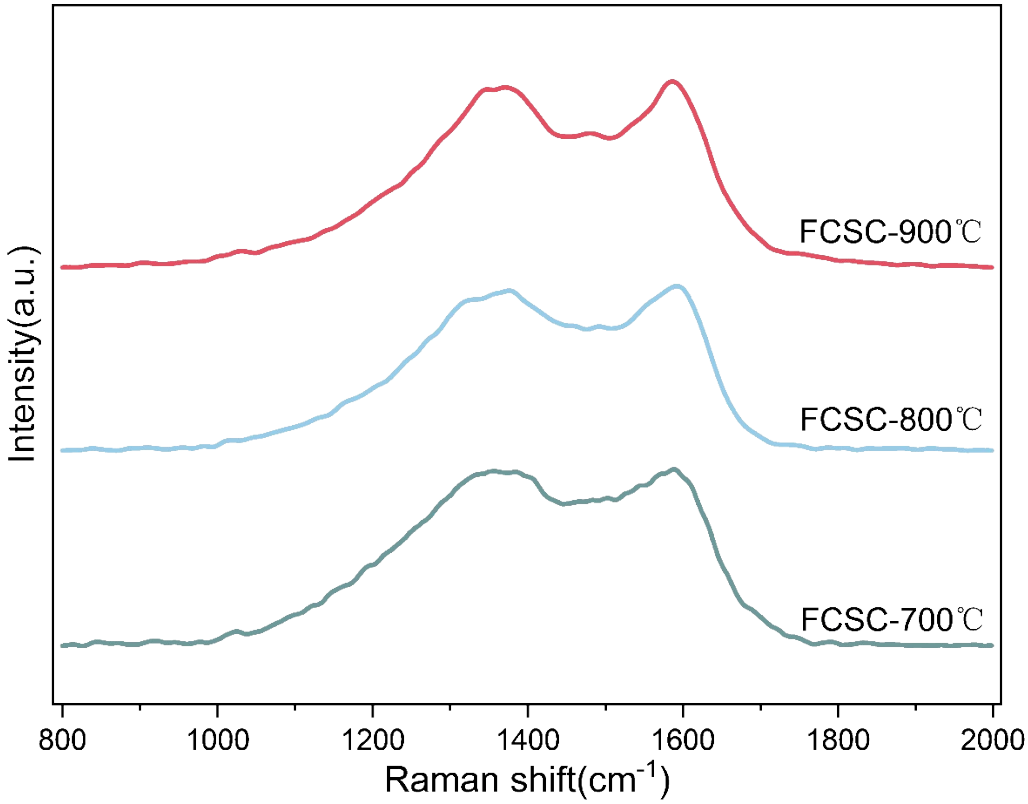

Figure S5. Raman parameters of the FCSC carbonized at different temperatures.

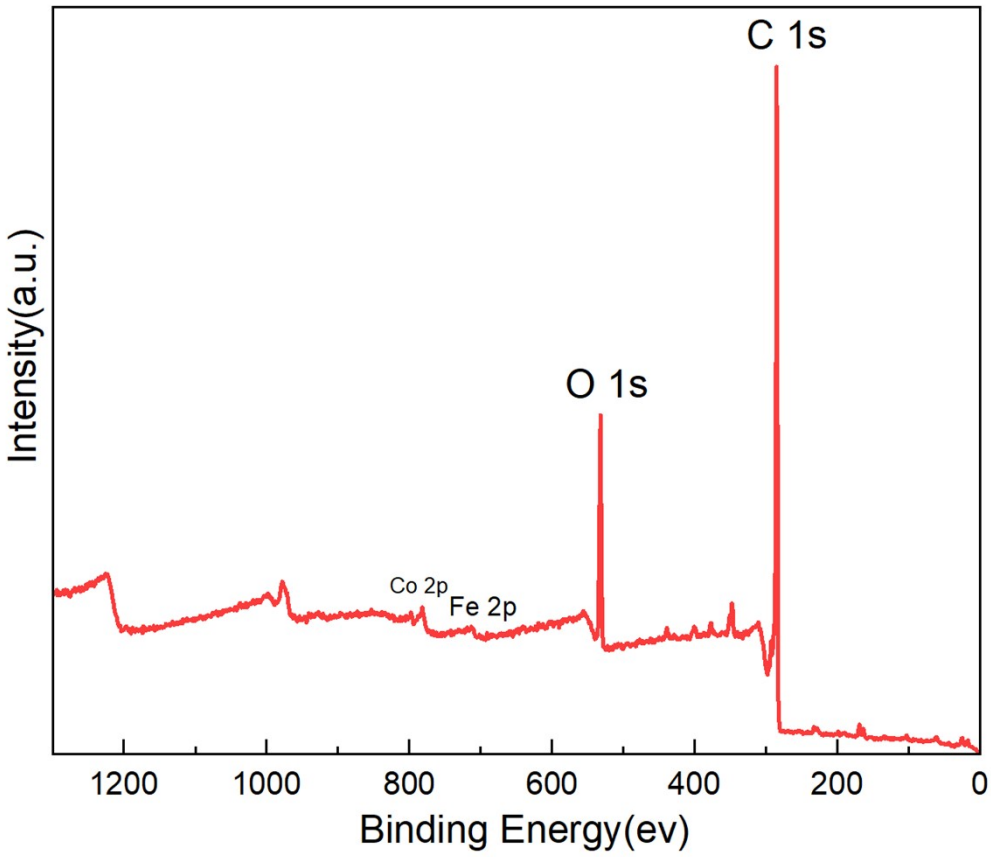

Figure S6. XPS spectra of the CFSC.

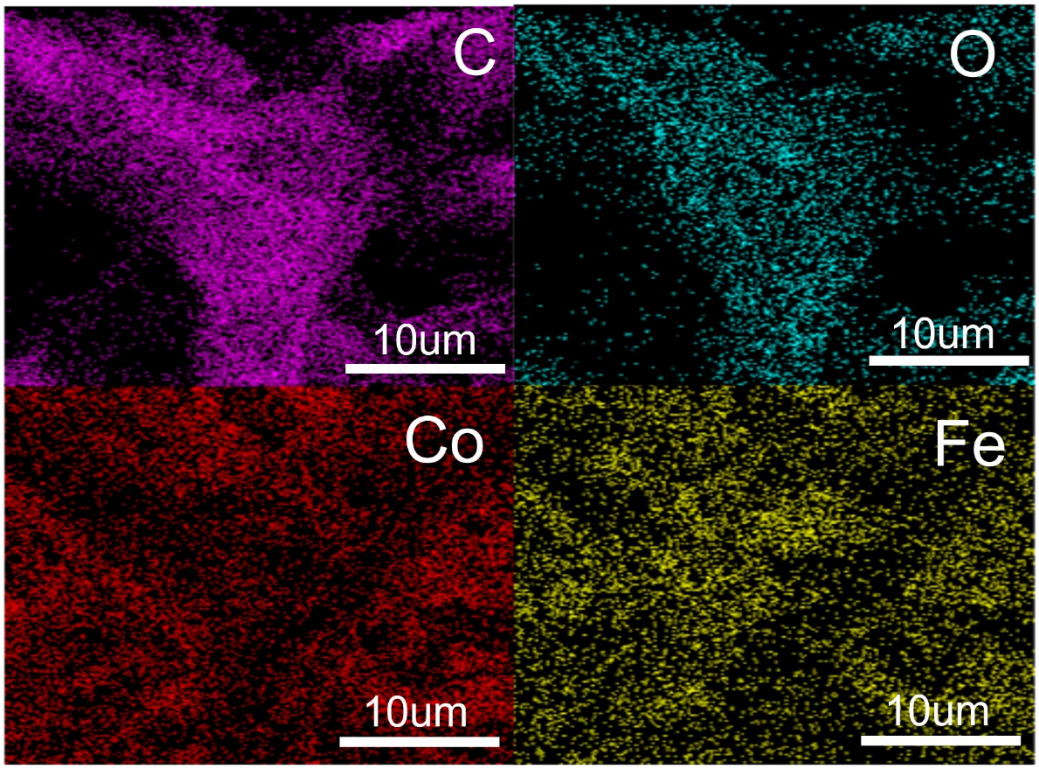

Figure S7. illustrates the elemental mapping spectra of FCSC.

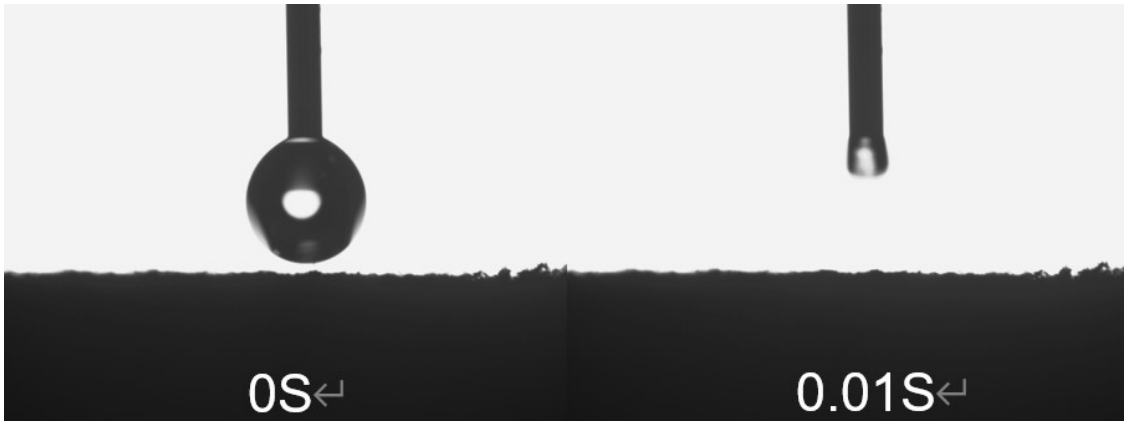

Figure S8. Contact-angle test of FCSC.

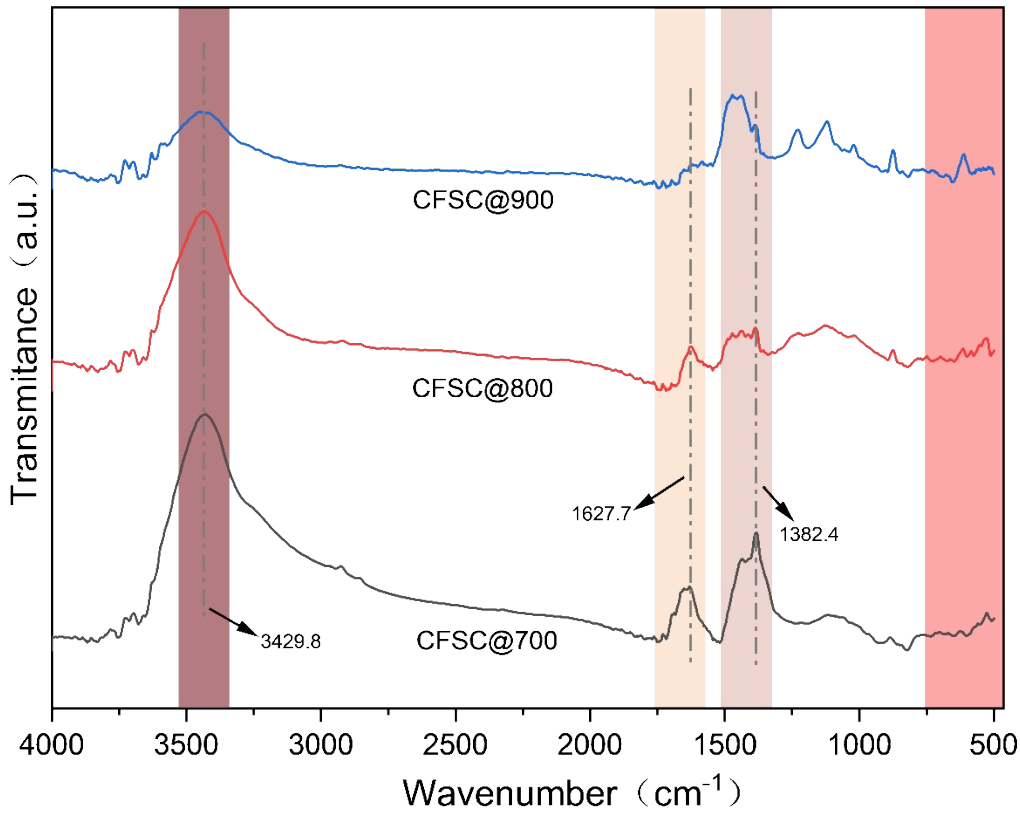

Figure S9. FTIR spectra at different firing temperatures.

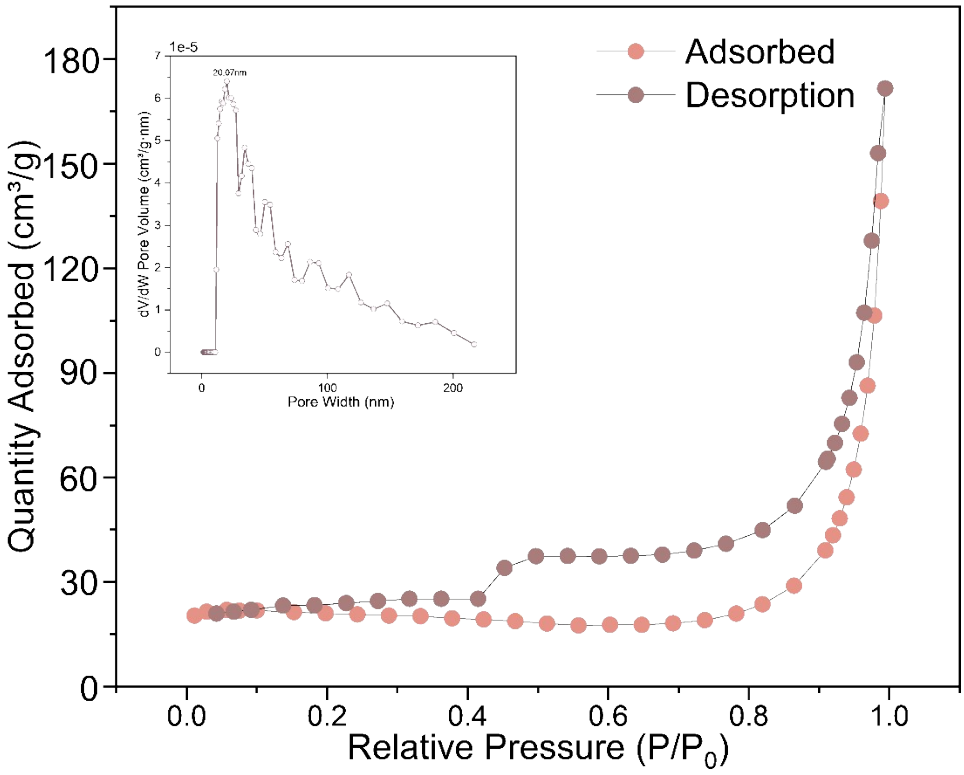

Figure S10. The nitrogen adsorption–desorption isotherms of the FCSC.

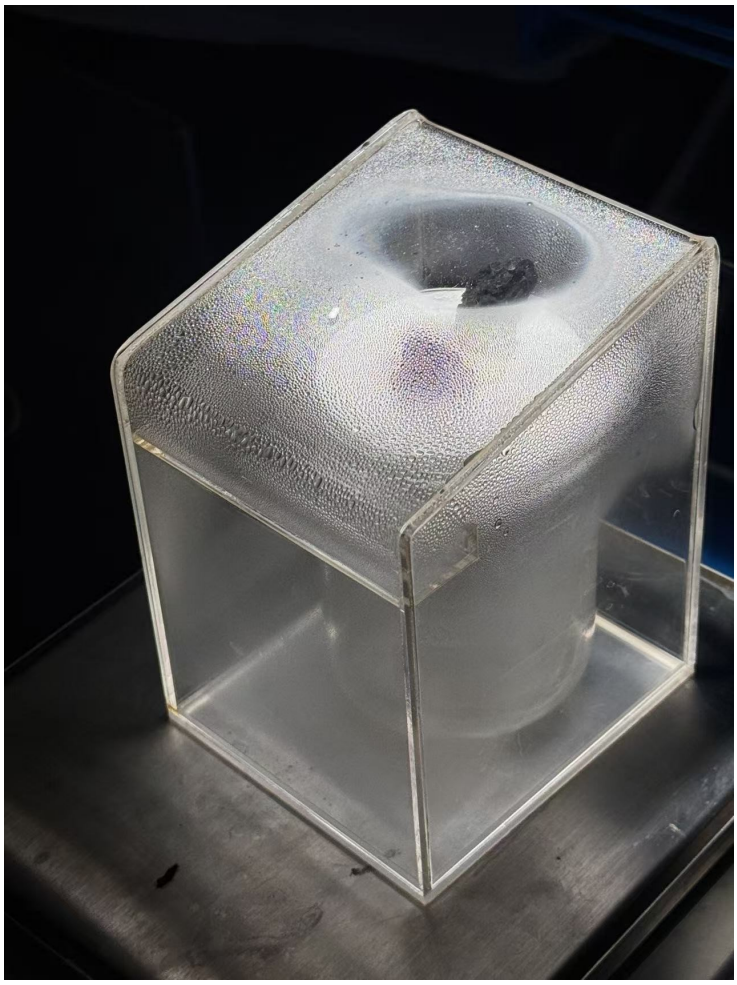

Figure S11. FCSC Evaporation Physical Diagram.

.

Figure S12. CFSC continuous evaporation10 day physical image.

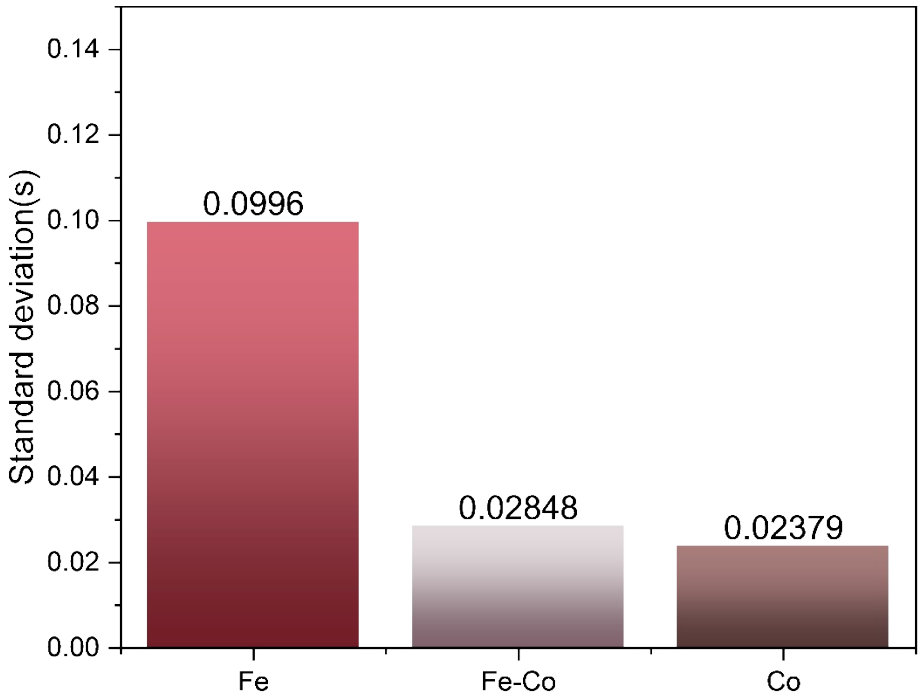

Figure S13. Fluctuation Differences Among Three Different PBAs During 10-Hour Evaporation.

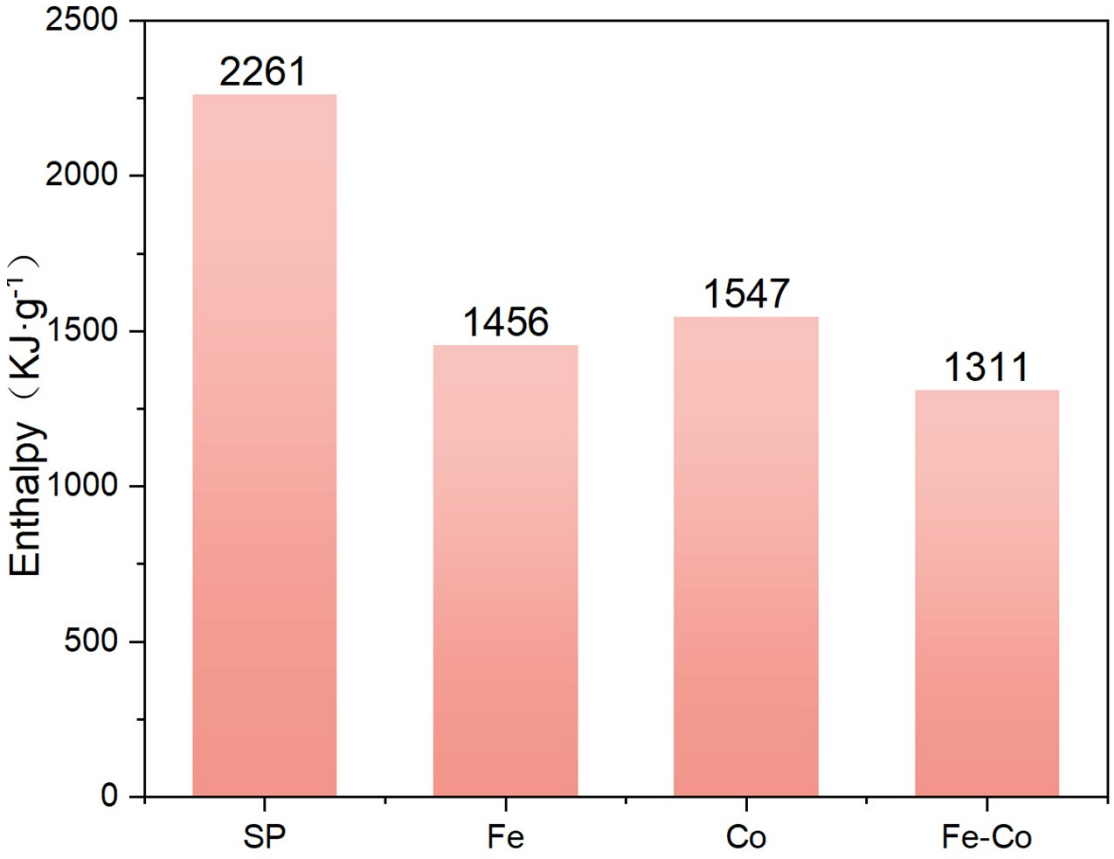

Figure S14. The equivalent enthalpy of evaporation of the material was calculated by the DSC method.

Figure S15. The decolorization experiments of FCSC for organic dyes.

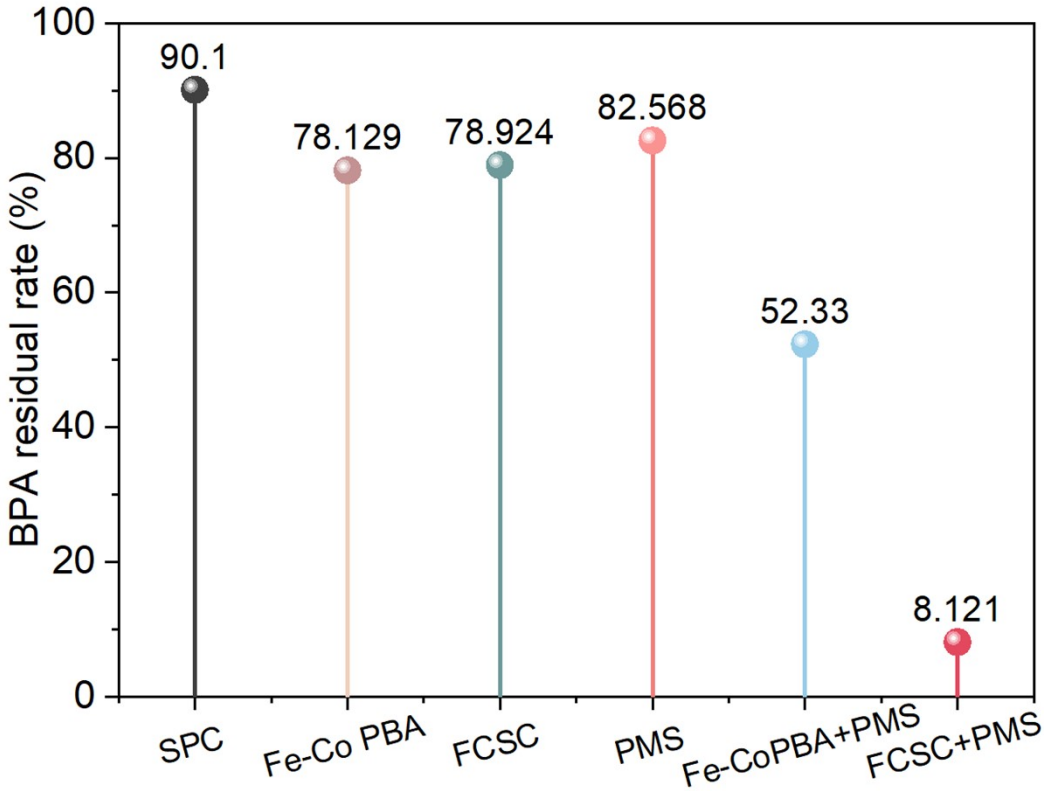

Figure S16. Efficiency of Different Materials in Adsorption and Degradation of Phenol.

Figure S17. Comparison of FCSC evaporation before and after ten hours.

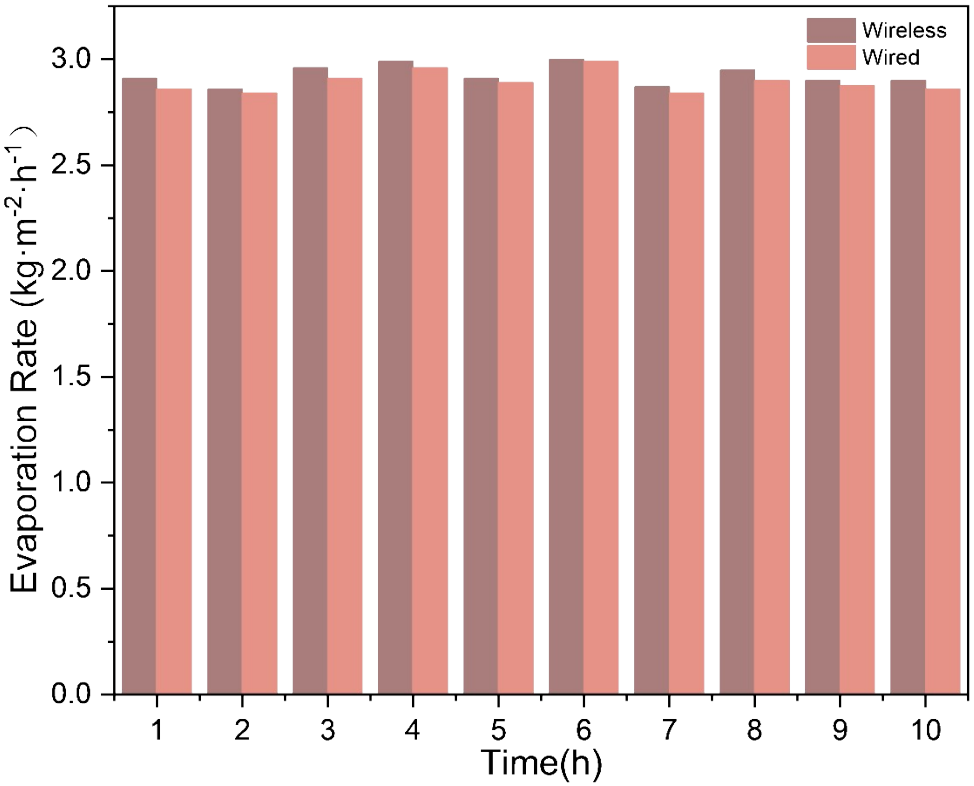

Figure S18. Comparison of Evaporation Rates with and without Wires.